Pharmaceutical Sciences Asia

Pharm Sci Asia 2025; 52(2), 240-249

DOI:10.29090/psa.2025.02.24.2601

Research Article

Soybean Oil in Nifedipine-Loaded Nanostructured Lipid Carriers: Enhancing Drug Loading and Release

Duangmanee Maneerojpakdee[1], Nattawat Natapulwat[2], Nuttanan Sinchaipanid[1,*]

[1] Department of Manufacturing Pharmacy, Faculty of Pharmacy, Mahidol University, Bangkok 10400, Thailand
[2] Department of Industrial Pharmacy, Faculty of Pharmacy, Silpakorn University, Nakhon Pathom 73000, Thailand

ABSTRACT

Nanostructured lipid carriers (NLCs) are widely recognized for their ability to improve drug loading (DL) capacity and release characteristics for poorly water-soluble drugs. In this study, nifedipine-loaded NLCs (NLC-NIs) were prepared using an ultrasonic emulsification method. The effects of dispersion energy and sonication time on the optimization of the preparation process were systematically investigated. The influence of soybean oil (SO) content, ranging from 5% to 25% w/w of the total lipid, on the physicochemical properties, entrapment efficiency (EE), and drug loading capacity (DL) was evaluated and compared with nifedipine-loaded solid lipid nanoparticles (SLN-NI). Results indicated that both %EE and %DL increased with higher SO concentrations. At the highest SO content, EE and DL were achieved at 97.66% ± 0.06 and 19.52% ± 0.01, respectively, while SLN-NI exhibited significantly different ($p < 0.05$) lower EE and DL values of 41.63% ± 0.10 and 8.32% ± 0.01, respectively. The particle size of NLC-NI 5 was 281.9 ± 16.4 nm, which was slightly larger with significantly different ($p < 0.05$) than that of SLN-NI (220.3 ± 14.5 nm). Additionally, NLC-NI demonstrated a superior sustained release profile in vitro compared to SLN-NI. In conclusion, the incorporation of SO in NLC formulations markedly improved drug EE, DL, and sustained release characteristics compared to solid lipid nanoparticles.

Keywords:
Nanostructured lipid carriers; Nifedipine; Solid lipid nanoparticles; Soybean oil; Ultrasonic emulsification method; Bioavailability enhancement; Drug delivery

1. INTRODUCTION

Solid lipid nanoparticles (SLNs) have been developed as an alternative carrier system to overcome the drawbacks associated with traditionally colloidal dispersions, such as physical stability, drug leakage during storage, protection of chemically labile drug molecules from environment and upscale production techniques[1,2]. They are sub-micron colloidal carriers dispersed either in water or in an aqueous surfactant solution, allowing the preparation to avoid any organic solvents. SLNs are simply prepared either with solid lipid, which are biocompatible and biodegradable, along with emulsifiers as stabilizing agents[3]. Thus, SLNs exhibit less acute and chronic toxicity than other polymeric nanoparticles. Furthermore, SLNs have the capability of modulating drug release, allowing both controlled and sustained release[4]. There are numerous types of solid lipid that have been studied, such as Compritol 888 ATO[5,6], glyceryl monostearate[7,8], stearic acid[9,10], trimyristin [11,12], Imwitor® 900[13,14] and Dynasan®[15]. SLNs have been shown to improve the bioavailability of poorly soluble drugs, including raloxifene[5], cannabidiol[8] and docetaxel[11]. However, there are some limitations of SLNs, such as drug loading capacity (DL) due to the solubility of drug in the solid lipid matrix, drug expulsion due to transformation into a crystalline structure, and the formation of a perfect crystal during storage[16].

To overcome these limitations of SLNs, nanostructured lipid carriers (NLCs) were developed as a new generation of lipid carriers[17]. NLCs are produced

***Corresponding author:**
* Nuttanan Sinchaipanid Email: nuttanan.sin@mahidol.ac.th

by controlled mixing of solid lipids and liquid lipids. Therefore, NLCs comprise different lipid molecules in the matrix. The differences in structure of solid and liquid lipids result in many imperfections in the matrix, which can accommodate drug in molecular form and thus prevent drug expulsion. Moreover, liquid lipids have a greater potential in solubilizing lipophilic molecules to enhance drug-loading capacity. For example, fluticasone loaded in NLCs composed of a mixture of precirol® ATO 5 and labrasol showed improved stability and loading capacity of the drug[18]. Docetaxel loaded NLCs composed of GMS, soyabean lecithin, stearic acid and oleic acid[19] exhibited sustained drug release profiles.

Nifedipine (NI) is a dihydropyridine calcium channel blocker widely used in treating hypertension, Prinzmetal's angina pectoris and other vascular disorders, such as Raynaud's phenomenon. This non-polar compound (log P = 2.50) has been reported to have low bioavailability (approximately 45–56%) and a short elimination half-life of around 2 hours.

Compared to mechanical agitation, the ultrasound technique at a low frequency was found to require less surfactant and lower energy consumption to produce less polydisperse and more stable nanoparticles within the same droplet size range[20]. The dispersion energy intensity and sonication time were examined to compare ultrasonic emulsification with rotor–stator dispersion, revealing that the ultrasound technique was more effective in reducing droplet size reduction[21].

Considering the advantages of NLCs prepared using ultrasonic techniques, this study aimed to explore the potential of soybean oil (SO) as a liquid lipid to overcome the limitations of SLNs. NI-loaded NLCs (NLC-NIs) containing varying concentrations of SO were developed and compared with NI-loaded SLNs (SLN-NI). In other study, NI loaded NLCs coated with Fenugreek Seed Polysaccharide were showed better stability and higher entrapment efficiency (EE)[22]. Thus, the NLCs system with varying compositions also presents a promising. The study also optimized dispersion energy and sonication time for lipid particles preparation. SO, a natural oil primarily composed of unsaturated fatty acids (linoleic and oleic acids), was selected for its biocompatibility and widespread availability. Poloxamer 188 (PO) and lecithin (LE) were used as emulsifiers in all formulations. Parameters including particle size, zeta potential, EE, DL, crystallinity, and *in vitro* release profiles were systematically investigated.

2. MATERIALS AND METHODS

2.1. Materials

NI (99 %) was purchased from Sharon Bio-medicine Ltd (Mumbai, India). Glyceryl palmitostearate (Precirol® ATO 5) (GP) was purchased from Gattefosse (Milan, Italy). SO and PO (Pluronic® F68) were purchased from Sigma-Aldrich (St. Louis, USA). LE was purchased from Union Chemical 1986 Co., Ltd. (Bangkok, Thailand). Treahalose was purchased from Hayashibara Co., Ltd. (Okayama, Japan).

2.2. Optimization of ultrasonic emulsification method

In order to select the dispersion energy and sonication time for preparation, a blank of NLC-NI 1 (bl NLC-NI 1) formula (Table 1) was chosen as it was the starting composition of NLC formulations (the lowest concentration of SO) and varying dispersion time for 2, 4, 6, 8 and 10 min at 10, 20, 30, 40 and 50 W [21]. Table 1 showed the formulas of NI-loaded and blank SLNs and NLCs system (w/w). The aqueous and lipid phases were separately prepared. Lipid phase consisting of GP, SO and LE was heated up to 75 ºC. Aqueous phase consisting of PO and sterile water for irrigation was also heated up to 75 ºC and then added to the molten lipid phase. The mixture was homogeneously stirred by a mechanical agitator (Model LMS 1003, Daihan labtech, kyonggi-do, Korea) for 900 s and then dispersed with an ultrasonic probe sonifier (Digital Sonifier® Model 250D, Branson Ultrasonics, Danbury, CT, USA). The bl NLC-NI 1 dispersion was placed at room temperature to cool down for 4 h and its particle size was determined by the particle size analyzer.

2.3. Preparation of SLN-NI and NLC-NIs formulations

SLNs and NLCs with different SO contents were prepared by the ultrasonic emulsification method. The mixture was ultrasonically emulsified at an optimized dispersion energy of 30 W for 2 min. The SO concentrations were increased until achieve almost 100% entrapment efficiency. The amounts of SO were varied from 5 – 25% w/w of total lipid in formulations. The formulas are shown in Table 1. The physicochemical characterization of NLC-NIs formulations and SLN-NI were determined.

2.4. Physicochemical characterizations of SLN-NI and NLC-NIs

2.4.1. Particle size and zeta potential analysis

The mean particle sizes, polydispersity index (PDI) and zeta potential of lipid nanoparticles were analyzed using Zetasizer ZS (Malvern Instruments, Worcestershire, UK). The intensity of laser light scattered by the samples was detected at an angel of 173º by the photomultiplier. The measurements were conducted in freshly prepared samples, at room temperature.

Table 1. Formulas of NLC-NIs, SLN-NI and blank SLNs and NLCs system (w/w)

Formulation	NI	GP	SO	LE	PO	Water qs to
bl NLC 1	-	4.75	0.25	0.5	2	100
NLC-NI 1	0.5	4.75	0.25	0.5	2	100
bl NLC 2	-	4.50	0.50	0.5	2	100
NLC-NI 2	0.5	4.50	0.50	0.5	2	100
bl NLC 3	-	4.25	0.75	0.5	2	100
NLC-NI 3	0.5	4.25	0.75	0.5	2	100
bl NLC 4	-	4.00	1.00	0.5	2	100
NLC-NI 4	0.5	4.00	1.00	0.5	2	100
bl NLC 5	-	3.75	1.25	0.5	2	100
NLC-NI 5	0.5	3.75	1.25	0.5	2	100
bl SLN	-	5.00	-	0.5	2	100
SLN-NI	0.5	5.00	-	0.5	2	100

SLN: Solid lipid nanoparticles; NLC: Nanostructured lipid carriers; NI: Nifedipine; GP: Glyceryl palmitostearate; SO: Soy bean oil; LE: Lecithin; PO: Poloxamer 188; bl NLC: Blank nanostructured lipid carriers; NLC-NI: Nifedipine-loaded nanostructured lipid carriers; bl SLN: Blank solid lipid nanoparticles; SLN-NI: Nifedipine-loaded solid lipid nanoparticles

2.4.2. EE and DL determinations

The EE of NI in lipid nanoparticles was determined indirectly by measuring the concentration of free drug in aqueous phase of the nanoparticle dispersion using ultrafiltration technique (Kubota Model 6930, Kubota Corporation, Bunkyo-ku, Tokyo). Five milliliters of undiluted nanoparticle dispersion were placed in the inner chamber of ultracentrifuge tube and centrifuged at 5000 rpm for 60 min. The sample (1 mL) in recovery chamber was withdrawn and transferred to 10 mL volumetric flask and then diluted to scale with mobile phase. The diluted sample was filtered through 0.22 µm membrane and NI concentration was determined by HPLC method. The EE and DL were calculated using equations as below.

$$EE(\%) = \frac{W_{total} - W_{free}}{W_{total}} \times 100 \quad (1)$$

$$DL(\%) = \frac{W_{total} - W_{free}}{W_{lipid}} \times 100 \quad (2)$$

where; W_{total}, W_{free} and W_{lipid} denoted the total amount of drug in system, the amount of free drug determined in the aqueous phase after the nanoparticles were separated and the weight of lipid nanoparticle, respectively.

2.4.3. Transmission electron microscopy (TEM)

The morphology of lipid nanoparticles was investigated using the TEM (Model JEM-2100, JEOL, Tokyo, Japan). The sample was prepared by placing a drop of dispersion onto a copper grid. The nanoparticles were negatively stained by using 1.5% (w/v) aqueous solution of phosphotungstic acid. The grid was then observed in a transmission electron microscope.

2.4.4. Freeze-drying of NI-loaded SLN and NLC

Trehalose was used in the freeze-drying process as a cryoprotectant at a concentration of 3% w/w. The lipid nanoparticle dispersion was pre-frozen using an ultra-cold freezer at -80 ºC for 24 h and the samples were then transferred to the freeze-dryer (Christ Alpha 1-2, GmbH, Osterode am Harz, Germany) for 36 h. The freeze-dried lipid nanoparticles were collected for DSC characterization and *in vitro* drug release studies.

2.4.5. Differential scanning calorimetry (DSC) analysis

DSC analysis was performed using differential scanning calorimeter (Model DSC 7, Perkin-Elmer, Norwalk, USA). The freeze-dried lipid nanoparticles were weighed accurately about 2-3 mg and placed in aluminium pans. The empty aluminium pan was used as a reference. The thermograms were run at a scanning rate of 5 ºC/min from 25 ºC to 200 ºC under a nitrogen purge.

2.4.6. X-ray diffraction analysis (XRD)

The crystalline state of the freeze-dried lipid nanoparticles was identified by the x-ray diffraction analysis (Model D8-Discover, Bruker, Madison, WI, USA). Diffractograms were performed from the initial angle $2\Theta = 3^o$ to the final angle $2\Theta = 60^o$. The data used were typically collected with a step width of 0.02^o and time/step = 6.00 s.

2.4.7. In vitro drug release study

A dissolution apparatus equipped with rotating paddles was employed for *in vitro* drug release study. NLC-NI 5 was selected for drug release comparison

with SLN-NI. Solubility of NI is 0.07 mg/ml[23]. The freeze-dried sample equivalent to 20 mg NI was exactly weighed and redispersed into 50 mL of the simulated intestinal fluid (SIF) with 1% sodium lauryl sulfate (SLS) then charged into dialysis bag and placed in 850 mL SIF with 1% SLS. The revolution speed of the paddle was set at 100 rpm and temperature was at 37 ± 0.5 ºC. Two milliliters of dissolution medium were withdrawn at the predetermined time intervals and the same volume of fresh dissolution medium was replenished. The samples were filtered through 0.22 µm membrane and NI concentration was then determined by HPLC method.

2.4.8. HPLC analysis of NI

The quantification of NI for EE and DL determinations and *in vitro* release study were performed using the HPLC method (Shimadzu-LC 20AD, Kyoto, Japan). The HPLC method was follow USP 2024 under Nifedipine monograph[24]. A Hypersil BDS column was employed for HPLC chromatographic separation at room temperature. The mobile phase consisted of a 25:25:50 (v/v/v) mixture of methanol:acetonitrile:water at a constant flow rate of 1.0 mL/min. The detection was carried out at 265 nm.

The analytical method for NI quantification was validated, covering linearity, precision, accuracy, limit of detection (LOD), limit of quantification (LOQ), and specificity. The method exhibited excellent linearity within the concentration range of 0.5 - 50 µg/mL, with a correlation coefficient (R^2) of 0.9998 and a regression equation of y = 19,981,406.4761x + 1,874.5939. Accuracy assessment showed recovery rates for spiked samples between 98.1–101.2%, confirming high accuracy. Precision analysis revealed intra-day and inter-day relative standard deviations (RSD) were the same value of 0.01%, satisfying the acceptable criterion of < 2%. The LOD and LOQ were determined to be 0.1 µg/mL and 0.4 µg/mL, respectively, using the signal-to-noise ratio method. Specificity testing confirmed no interference from excipients or degradation products in chromatograms. These results confirm the method's reliability for NI quantification.

2.4.9. Statistical analysis

All experiments were performed in triplicate, and all results were expressed as mean ± SD. Statistical analysis was carried out using SPSS 17.0 for Windows. Significant differences ($p < 0.05$) between means were assessed by one-way analysis of variance (ANOVA), followed by Tukey's honesty significant difference test.

3. RESULTS

3.1. Optimization of dispersion energy and sonication time

By emulsification method, the dispersion energy and sonication time were determined using bl NLC-NI 1 as the base formulation. The size of bl NLC-NI 1 decreased with the increased dispersion energy and sonication time as shown in **Figure 1.** However, the particle sizes forming at 30, 40 and 50 W were not significantly different when varying sonication time from 2 to 10 min. It could be explained that the droplet size passed through a minimum size at an intermediate power application and then constant or slightly increased at higher power level, i.e., at the dispersion

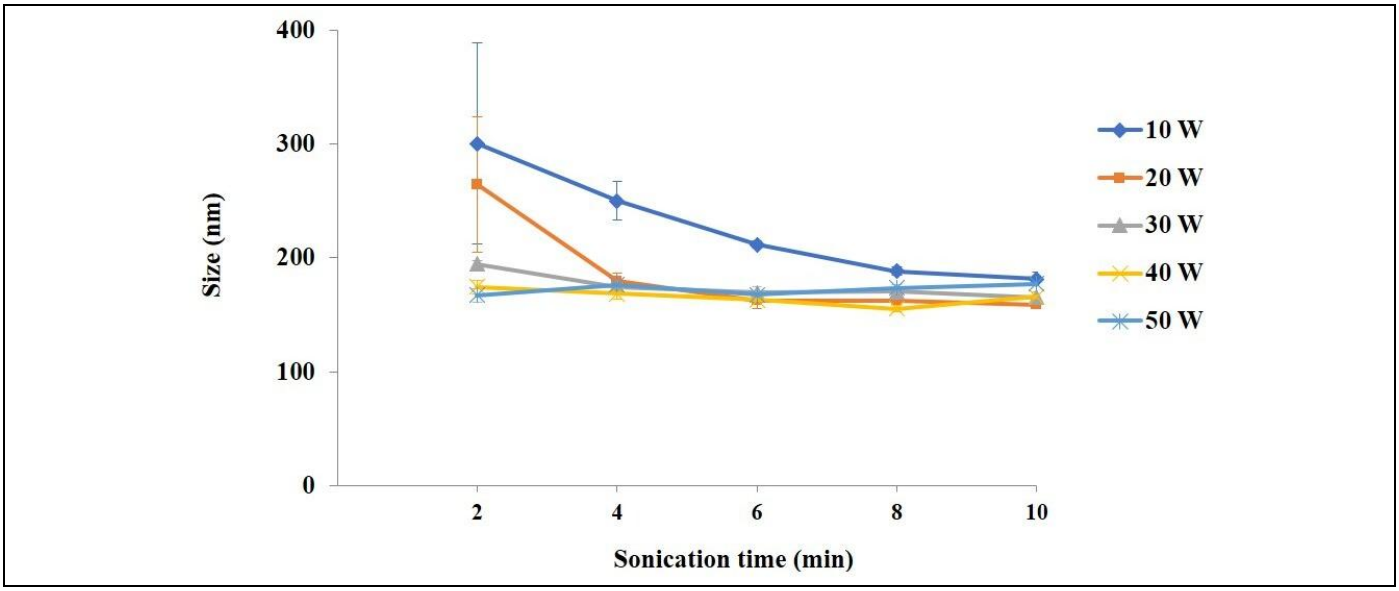

Figure 1. The effects of the dispersion energy and sonication time on the particle size of bl NLC-NI 1. Error bar stands for SD (n=3).

energy of 40 and 50 W for 10 min. This effect has been described as over-processing which is caused by an increase in emulsion droplet coalescence at the higher energy input[25]. The high intensity combined with higher rate of collision may cause drop breakage resulting in increasing droplet coalescence. Furthermore, understanding the interplay between sonication parameters and particle size can aid in the rational design of nanostructured lipid carriers with made-to-measure properties for specific drug delivery applications, ensuring efficient drug encapsulation and controlled release profiles. **Figure 1.** demonstrated that the dispersion energy of 30 W was able to reduce droplet size at the shortest sonication time. Additional dispersion energy and sonication time provided no greater reduction in droplet size. Therefore, in this study the dispersion energy and sonication time used for the SLN-NI and NLC-NIs preparations were 30 W and 2 min, respectively.

3.2. Physicochemical properties of SLN-NI and NLC-NIs

3.2.1. Particle size and zeta potential analysis

The mean particle size, polydispersity index (PDI) and zeta potential of SLN-NI and NLC-NIs were shown in Table 2. The particle sizes of all formulations were in the size range of between 200 to 300 nm. This size range is appropriate for oral dosage form because the normal epithelial cells can up-take in particle size range < 300 nm[26]. Furthermore, it had a trend towards bigger particle size with increasing SO content. The PDI generally describes the deviation of the measured autocorrelation function from that of a dispersion of monodisperse spheres with the same diameter. The PDI values in the range 0.01 - 0.5 indicate monodisperse particles, whereas PDI values > 0.7 indicate a polydisperse distribution[27]. All formulations provided PDI < 0.5 representing a relatively narrow size distribution. Physical stability can be predicted by measuring the zeta potential. Mostly, high negative or positive charge can prevent aggregation of the particles due to their high repulsion[28,29]. All zeta potential values were not significantly different ($p < 0.05$) between all formulations. The zeta potential values were between -45.5 mV and -25.3 mV which would be achieved good stability and dispersion.

The findings underline the critical nature of particle size, PDI, and zeta potential in assessing the physicochemical characteristics of SLN-NI and NLC-NIs formulations. The optimal particle size range ensures enhanced cellular uptake, crucial for effective oral delivery[30]. Furthermore, the uniform size distribution as indicated by the PDI values suggests a consistent formulation quality, which is essential for achieving predictable pharmacokinetics and drug release profiles. Similarly, the zeta potential values obtained suggest that the formulations possess desirable stability attributes, mitigating the risk of particle aggregation.

3.2.2. EE and DL determinations

Since liquid lipids in the NLCs formulations help promote solubilization of lipophilic molecules to a much higher extent than solid lipids, the NLCs would provide a higher incorporation capacity of lipophilic drug in the matrix with sustained release property. Therefore, the amount of liquid lipid would be the major factor affecting the EE and DL of NLC-NIs[31]. The EE of formulations with different SO concentrations (5, 10, 15, 20 and 25% w/w of total lipid) are also shown in Table 2. EE and DL increased with the increased SO concentration. %EE and %DL of NLC-NI 5 was 97.66% ± 0.06 and 19.52% ± 0.01, respectively exhibiting the highest EE and DL values compared to SLN-NI that exhibited the lowest ones at 41.63% ± 0.10 and 8.32% ± 0.01, respectively.

The high %EE and %DL achieved with 25% w/w SO concentration indicate an optimal balance between the liquid and solid lipids, maximizing drug incorporation while maintaining the structural integrity necessary for sustained release.

3.2.3. TEM

The morphological images of SLN-NI and NLC-NIs were shown in **Figure 2.** Different morphology of lipid nanoparticles was reported using different microscopes. The SLN-NI and NLC-NIs had spherical shape using TEM[32]. The observed particle sizes in all formulations were in the range of 200 to 300 nm, which were similar to the size range measured by Zetasizer ZS.

Table 2. The particle size, PDI, zeta potential, EE (%) and DL (%) of the SLN-NI and NLC-NIs, each value represents the mean ± S.D. (n=3)

Formulation	Particle size (nm)	PDI	Zeta potential (mV)	EE (%)	DL (%)
NLC-NI 1	228.0 ± 12.1 [a]	0.380 ± 0.007 [a, b]	-35.8 ± 9.0 [a]	74.31 ± 0.07 [b]	14.81 ± 0.01 [b]
NLC-NI 2	224.6 ± 12.6 [a]	0.387 ± 0.006 [a, b]	- 36.9 ± 8.5 [a]	85.91 ± 0.13 [b]	17.10 ± 0.01 [a, b]
NLC-NI 3	233.8 ± 11.4 [a]	0.394 ± 0.017 [a, b]	-36.4 ± 7.8 [a]	84.58 ± 0.15 [b]	17.14 ± 0.02 [a, b]
NLC-NI 4	240.9 ± 13.2 [a]	0.355 ± 0.050 [a]	- 35.4 ± 5.8 [a]	92.33 ± 0.08 [b]	18.45 ± 0.01 [b]
NLC-NI 5	281.9 ± 16.4 [b]	0.344 ± 0.048 [a, b]	-35.2 ± 7.2 [a]	97.66 ± 0.06 [b]	19.52 ± 0.01 [b]
SLN-NI	220.3 ± 14.5 [a]	0.407 ± 0.024 [b]	-34.5 ± 9.2 [a]	41.63 ± 0.10 [b]	8.32 ± 0.01 [b]

PDI: Polydispersity index; EE: Entrapment efficiency ; DL: Drug loading capacity; SLN-NI: Nifedipine-loaded solid lipid nanoparticles; NLC-NIs: Nifedipine-loaded nanostructured lipid carriers 1 – 5; a: Not significantly difference; b: Significantly difference ($p < 0.05$)

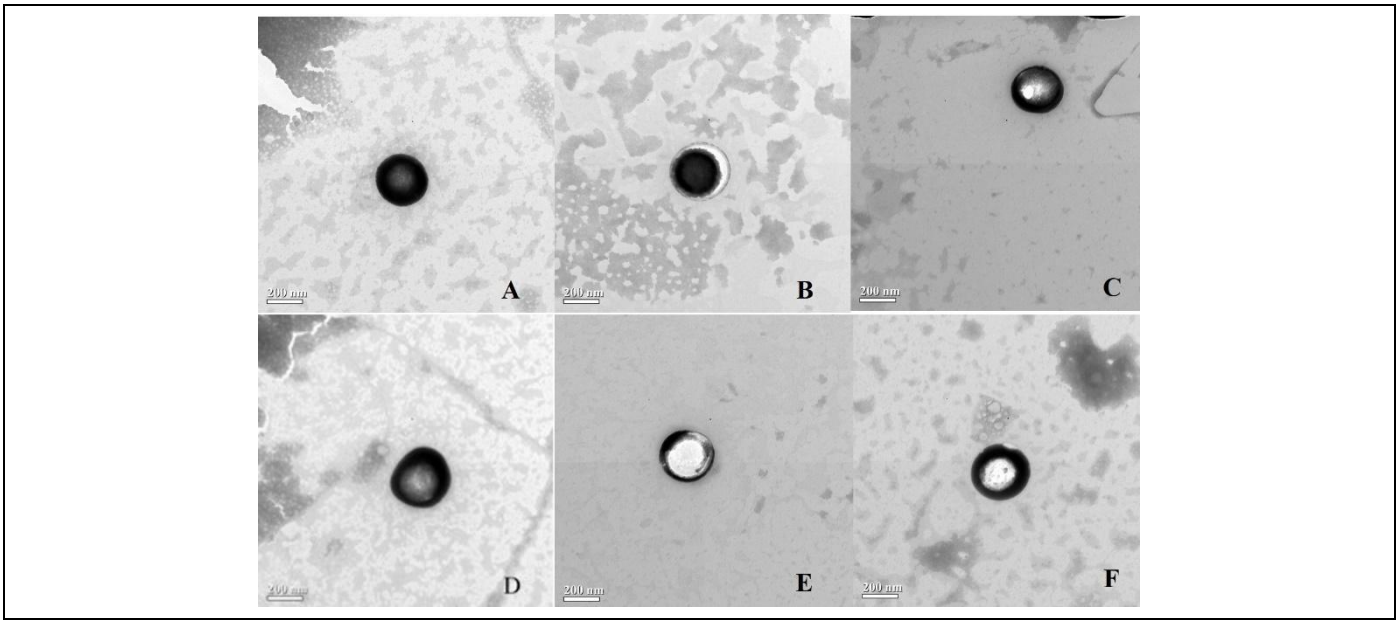

Figure 2. TEM morphology of A: SLN-NI; B: NLC-NI 1; C: NLC-NI 2; D: NLC-NI 3; E: NLC-NI 4; F: NLC-NI 5. Bar = 200 nm.

The consistency in particle size measurements obtained from both TEM and Zetasizer ZS underscores the reliability and accuracy of the particle size determination methods used in this study. The spherical morphology observed for both SLN-NI and NLC-NIs are indicative of a uniform and well-formed nanoparticle structure, which is crucial for predictable drug release profiles[30].

3.2.4. DSC analysis

DSC analysis was performed to obtain the thermograms of freeze-dried bl SLN, bl NLCs, SLN-NI and NLC-NIs compared to those of GP, PO and NI as shown in **Figure 3.** Using the DSC thermograms, changes in melting point and enthalpy could be investigated to demonstrate lipid modifications in NLC-NIs and SLNs. The melting peak of GP was shown at 58.3 °C, whereas it was shifted to 53.4 °C in SLNs and NLC-NIs. The observed shifts in melting points and the disappearance of the NI peak in the DSC thermograms provide critical insights into the structural transformations occurring within the lipid nanoparticles. The shift in the melting peak of GP and the depression in melting points of SLN-NI and NLC-NIs can be attributed to the reduction in particle size and the increased surface area, which enhances the interaction between the lipids and surfactants. This interaction can disrupt the crystalline structure, leading to a lower melting point as described by the Thomson equation[33,34].

The surfactants in these formulations might cause the crystal distortion and subsequently, melting points depression. The melting peak of NI was shown at 174.7°C which was disappeared in the DSC thermogram

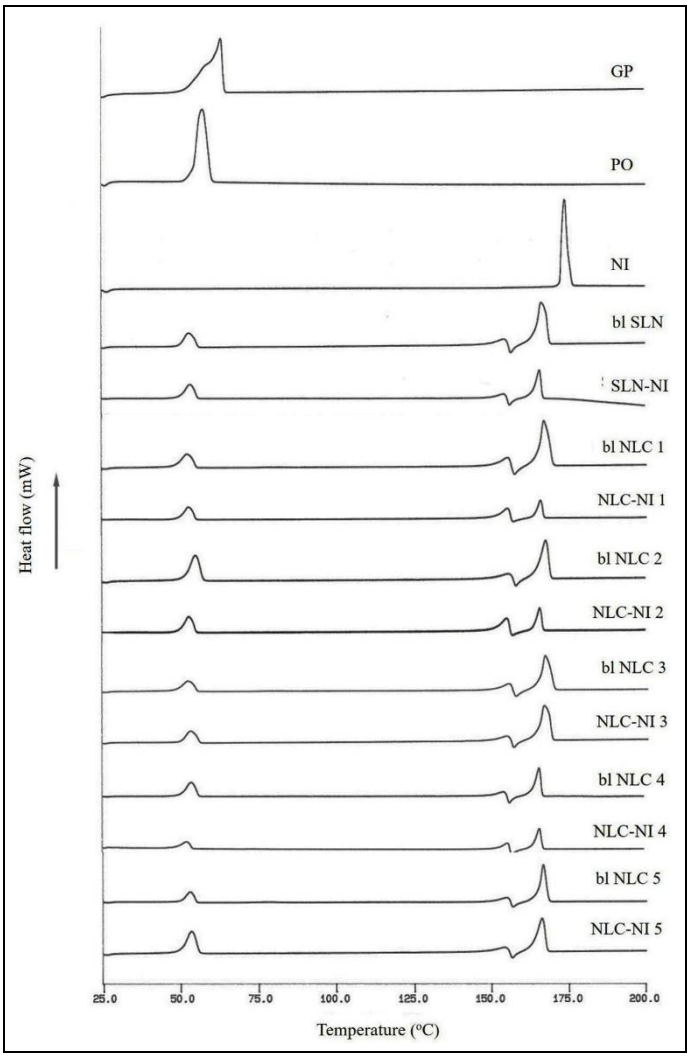

Figure 3. DSC thermograms of GP: Glyceryl palmitostearate, PO: Poloxamer 188, NI: Nifedipine, bl SLN: Blank solid lipid nanoparticles, SLN-NI: Nifedipine-loaded solid lipid nanoparticles, bl NLC 1-5: Blank nanostructured lipid carriers 1 - 5, NLC-NI 1 - 5: Nifedipine-loaded nanostructured lipid carriers 1 – 5.

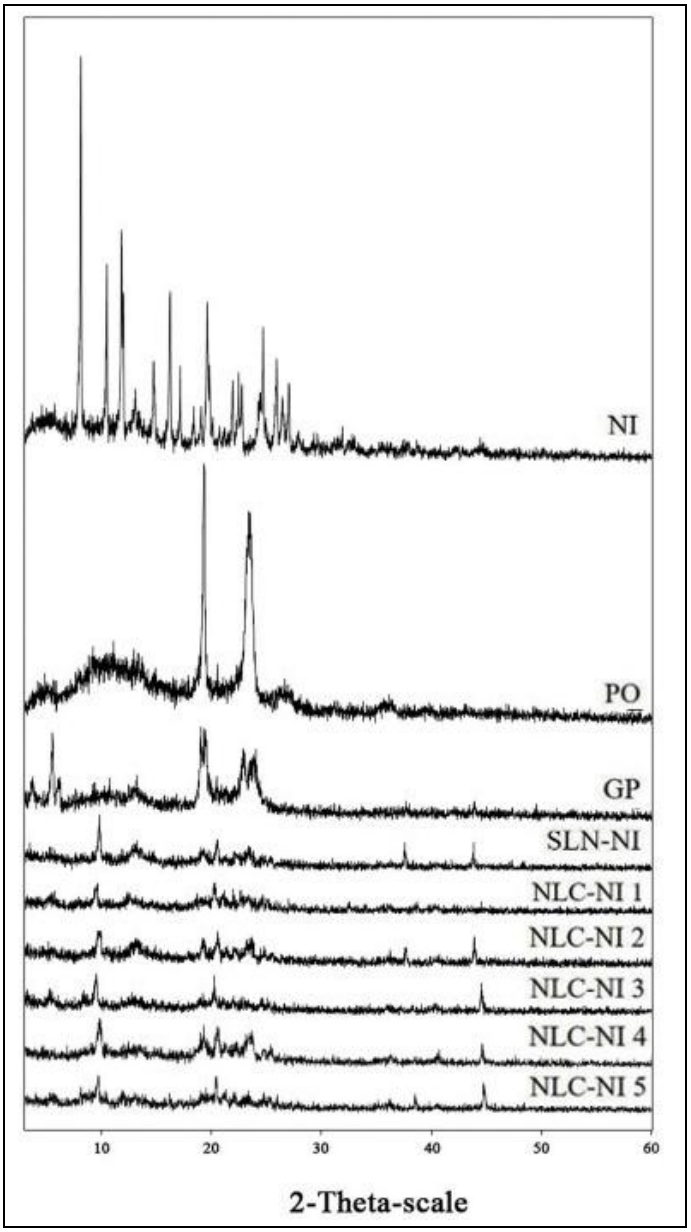

Figure 4. X-ray powder diffractograms of freeze-dried SLN and NLCs and their compositions. NI: Nifedipine, PO: Poloxamer 188, GP: Glyceryl palmitostearate, SLN-NI: Nifedipine-loaded solid lipid nanoparticles, NLC-NI 1 - 5: Nifedipine-loaded nanostructured lipid carriers 1 – 5.

of all freeze-dried formulations. These results indicated that NI was dissolved and stated in the amorphous form[35]. The complete dissolution of NI and its transition to an amorphous form within the freeze-dried formulations suggest a homogeneous distribution of the drug within the lipid matrix, which is crucial for achieving consistent drug release profiles. On the other hand, the new characteristic peak appeared at 160.7 °C as shown in **Figure 3.** This may result from the complexity further increased due to various lipids which had different melting enthalpy and the interactions of the lipid with the emulsifiers or corresponded to crystal lattice of the SLNs or NLCs particles[36].

3.2.5. XRD

The x-ray diffractograms of freeze-dried SLN-NI and NLC-NIs were compared to those of GP, PO and NI as shown in **Figure 4.** NI showed characteristic sharp peaks indicating the crystalline nature of the drug. On the contrary, the NI peaks were almost absent in freeze-dried SLN-NI and NLC-NIs indicating that NI was not in the crystalline form[37]. These results were in good agreement with the results obtained from DSC analysis. The absence of sharp NI peaks in the freeze-dried SLN-NI and NLC-NIs confirms that the drug is predominantly in an amorphous state, which is beneficial for enhancing its solubility and bioavailability.

The intensities and positions of GP and PO peaks in the x-ray diffractograms also changed due to the less ordered structure and pronounced crystal defects[38]. These results indicated that the degree of the crystallinity was lower in the freeze-dried SLN-NI and NLC-NIs than in the pure lipids. Furthermore, the peak intensities of NLC-NIs were less pronounced in comparison with that of SLN-NI, indicating that the degree of crystallinity in NLC-NIs was lower. The lower degree of crystallinity in NLC-NIs compared to SLN-NI further highlights the impact of liquid lipids in promoting an amorphous state and enhancing drug encapsulation efficiency. The reduced crystallinity not only aids in better drug solubilization but also contributes to the sustained release properties observed in NLC formulations. These findings underscore the importance of controlling the crystalline structure in lipid nanoparticles to optimize drug delivery performance.

3.2.6. In vitro drug release study

Figure 5. showed *in vitro* drug release profiles of NI from the SLN-NI and the NLC-NI 5 in SIF with 1% SLS. A biphasic release was observed in SLN-NI with rapid release up to 3 h followed by sustained release until 24 h whilst initial burst release was not observed in NLC-NI 5. The observed biphasic release profile in SLN-NI can be attributed to the initial release of surface-bound drug molecules followed by a slower diffusion-controlled release from within the solid lipid matrix. In contrast, the absence of an initial burst release in NLC-NI 5 highlights the homogenous distribution of NI within the lipid matrix, preventing surface crystallization and promoting a more controlled release. This finding is corroborated by X-ray diffraction and DSC analyses, which confirmed the amorphous state of NI in the NLCs formulation. Only 30.6 % of drug released from the NLC-NI 5 whilst 69.2 % of drug released from SLN-NI after 3 hours. Due to the crystal

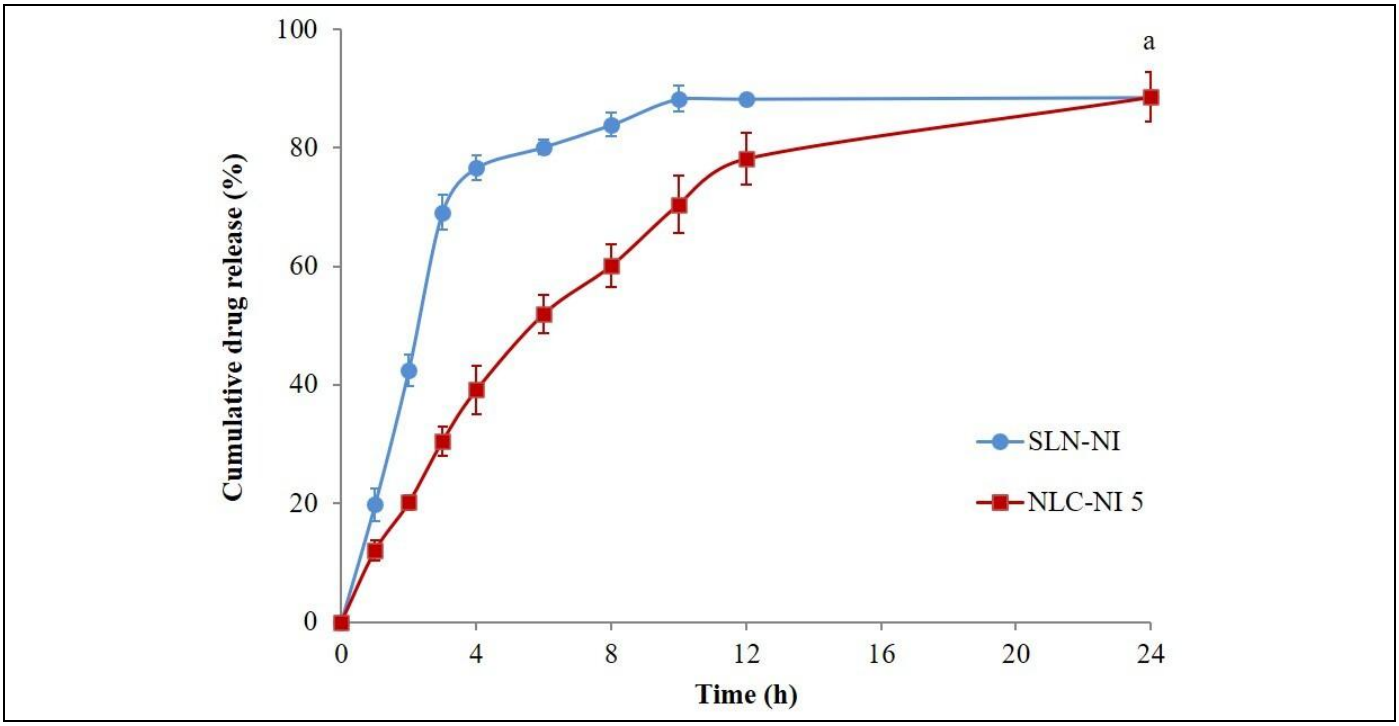

Figure 5. *In vitro* drug release profiles of SLN and NLC-NI 5 in SIF with 1% SLS (pH 6.8). Each value represents the mean ± SD (n = 3).
a: Not significantly difference

lattice structure of SLNs, drug might migrate easier than NLCs formulation resulting in faster drug release[39,40].

The drug release profiles of NLC-NI 5 showed the better sustained release pattern compared to those of SLN-NI. The superior sustained release profile of NLC-NI 5 suggests that the less ordered, more amorphous structure of NLCs effectively traps the drug within the lipid matrix, allowing for a more gradual and prolonged release.

4. CONCLUSION

SLNs and NLCs have demonstrated significant potential as advanced drug delivery systems for various therapeutic applications. NLCs are generally preferred due to their superior DL and controlled drug release profile. In this study, we evaluated NLCs formulated with SO as the liquid lipid and compared their performance with SLNs for NI delivery. Both SLN-NI and NLC-NIs exhibited spherical morphology, with small particle size, narrow PDI and zeta potential values indicative of good stability. Furthermore, all formulations-maintained NI in an amorphous state, suggesting that these systems can enhance the solubility of poorly water-soluble drugs. SLN-NI exhibited the lowest %EE and %DL values. However, as the SO content increased in NLC-NIs, %EE and %DL values improved. The highest SO content achieved %EE (97.66 ± 0.06%) and %DL (19.52 ± 0.01%), which also demonstrated a sustained release pattern in the *in vitro* release study. These findings indicate that incorporating SO into NLCs significantly enhances %EE, %DL, and drug release behavior for NI delivery. Further stability studies should be conducted to confirm the zeta potential results and validate the long-term viability of these formulations.

5. ACKNOWLEDGEMENTS

The authors would like to express deep gratitude to Ampol Mitrevej for his conceptual development, supervision and funding acquisition. In addition, the authors would like to thank Opa Vajragupta and Simon Knight for their extensive English revision.

Ethics approval
none to declare.

Conflict of interest
none to declare.

Funding
This research was funded by Thailand Research Fund through Royal Golden Jubilee Ph.D.Program, grant number PHD/0114/2548.

Author contribution
Conceptualization, D.M., N.N., and N.S.; methodology, D.M.; validation, D.M., N.N., and N.S.; formal analysis, D.M.; investigation, D.M.; resources, D.M.; data curation, D.M. and N.S.; writing—original draft preparation, D.M.; writing—review and editing, N.S.;

supervision, N.S.; funding acquisition, N.S. All authors have read and agreed to the published version of the manuscript.

Article info:
Received July 19, 2024
Received in revised form November 28, 2024
Accepted December 9, 2024

REFERENCES

1. Shidhaye SS, Vaidya R, Sutar S, Patwardhan A, Kadam VJ. Solid lipid nanoparticles and nanostructured lipid carriers - innovative generations of solid lipid carriers. Curr. Drug Del. 2008;5(4):3324-31.
2. Muchow M, Maincent P, Müller RH. lipid nanoparticles with a solid matrix (SLN®, NLC®, LDC®) for oral drug delivery. Drug Dev. Ind. Pharm. 2008;34(12):1394-405.
3. Müller RH. Lipid nanoparticles: Recent advances. Adv. Drug Deliv. Rev. 2007;59(6):375-76.
4. Das S, Chaudhury A. Recent advances in lipid nanoparticle formulations with solid matrix for oral drug delivery. AAPS. PharmSciTech. 2011;12:62–76.
5. Pant NC, Juyal V. *In-vitro* release and stability studies of raloxifene loaded solid-lipid nanoparticle. J. Pharm. Res. Int. 2021;33(39B):243–9.
6. Rao H, Ahmad S, Madni A, Rao I, Ghazwani M, Hani U, et al. Compritol-based alprazolam solid lipid nanoparticles for sustained release of alprazolam: Preparation by hot melt encapsulation. Molecules. 2022;27(24):8894.
7. Sabry SA, Abd El Razek AM, Nabil M, Khedr SM, El-Nahas HM, Eissa NG. Brain-targeted delivery of valsartan using solid lipid nanoparticles labeled with rhodamine B; a promising technique for mitigating the negative effects of stroke. Drug Del. 2023;30(1): 2179127.
8. Alcantara KP, Malabanan JWT, Nalinratana N, Thitikornpong W, Rojsitthisak P, Rojsitthisak P. Cannabidiol-loaded solid lipid nanoparticles ameliorate the inhibition of proinflammatory cytokines and free radicals in an *in vitro* inflammation-induced cell model. Int. J. Mol. Sci. 2024;25(9):4744.
9. Talele P, Jadhav A, Tayade S, Sahu S, Sharma KK, Shimpi N. Hydroquinone loaded solid lipid nanoparticles comprised of stearic acid and ionic emulsifiers: physicochemical characterization and *in vitro* release study. J. Mol. Liq. 2022;368:120590.
10. Khan H, Nazir S, Farooq RK, Khan IN, Javed A. Fabrication and assessment of diosgenin encapsulated stearic acid solid lipid nanoparticles for its anticancer and antidepressant effects using *in vitro* and *in vivo* models. Front. Neurosci. 2022;15:806713.
11. Dawoud M, Mojally M, Abdou R, Attia HG.. Comparative study on the performance of monoolein cubic nanoparticles and trimyristin solid lipid nanoparticles as carriers for docetaxel. Pharm. Dev. Tech. 2023;*28*(3–4):277–87.
12. Manjunath K, Venkateswarlu V. Pharmacokinetics, tissue distribution and bioavailability of clozapine solid lipid nano-particles after intravenous and intraduodenal administration. J. Control Release. 2005;107:215–28.
13. Heba E, Helen C, Edyta N, Cameron H, Keith A, Steve R, et al. High drug loading solid lipid nanoparticles, nanostructured lipid carriers and nanoemulsions for the dual drug delivery of the HIV drugs darunavir and ritonavir, JCIS Open. 2023;11:100087
14. Venkatesan K, Dutta G, Narayanaswamy D, Sugumaran A. development and optimization of candesartan cilexetil loaded solid lipid nanoparticles. Int. J. Pharm. Investig. 2023;13(4):754–62.
15. Niharika GM, Kannan K. Solid lipid nanoparticles of rebamipide: formulation, characterization and in vivo pharmacokinetic evaluation. Int. J. App. Pharm. 2022;14(2):143–50.
16. Müller RH, Radtke M, Wissing SA. Nanostructured lipid matrices for improved microencapsulation of drugs. Int. J. Pharm. 2002;242(1–2):121–28.
17. Viegas C, Patrício AB, Prata JM, Nadhman A, Chintamaneni PK, Fonte P. Solid lipid nanoparticles vs. nanostructured lipid carriers: A comparative review. Pharmaceutics. 2023;15(6):1593.
18. Doktorovová S, Araújo J, Garcia ML, Rakovský E, Souto EB. Formulating fluticasone propionate in novel PEG-containing nanostructured lipid carriers (PEGNLC). Colloids Surf. B Biointerfaces. 2010;75:538–42.
19. Liu D, Liu Z, Wang L, Zhang C, Zhang N. Nanostructured lipid carriers as novel carrier for parenteral delivery of docetaxel. Colloids Surf. B Biointerfaces. 2011;85:262–9.
20. Tadros T, Izquierdo P, Esquena J, Solans C. Formation and stability of nano-emulsions. Adv. Colloid Interface Sci. 2004;108-109:303-18.
21. Ahmed T, Eman A, Amr I, Muthupandian A, Xiaoyun X, Siyi P, et al. Ultrasonic emulsification: An overview on the preparation of different emulsifiers-stabilized emulsions. Trends Food Sci. Technol. 2020;105:363-77.
22. Arora SC, Anuradha K, Chahat S, Renu R. Formulation and characterization of nifedipine loaded nanostructured lipid carriers coated with fenugreek seed polysaccharide. Int. J. Sci. Res. 2019;9(11):103-7.
23. Bhaskar R, Parjane R, Ola M, Singh B, Srivastava N, Gupta R. Design, development and biological evaluation of nifedipine-loaded oral film in the management of cardiovascular diseases. Biochem. Cell. Arch. 2024;24:653-61.
24. United States Pharmacopeial Convention. Nifedipine. In: United States Pharmacopeia 2024/National Formulary 39. Rockville, MD: United States Pharmacopeial Convention; 2024.
25. Jafari SM, He Y, Bhandari B. Nano-emulsion production by sonication and microfluidization - a comparison. Int. J. Food Prop. 2006;9:475−85.
26. Shah RM, Rajasekaran D, Ludford-Menting M, Eldridge DS, Palombo E.A, Harding IH. Transport of stearic ac-id-based solid lipid nanoparticles (SLNs) into human epithelial cells. Colloids Surf. B Biointerfaces. 2016;140:204-12.
27. Kumar R, Kumar S, Sinha VR. Evaluation and optimization of water in oil microemulsion using ternary phase diagram and central composite design. J. Dispers. Sci. Technol. 2015;3:37–41.
28. Freitas C, Müller RH. Effect of light and temperature on zeta potential and physical stability in solid lipid nanoparticle (SLN) dispersions. Int. J. Pharm. 1998;168(2):221–9.
29. Rizwanullah M, Amin S, Ahmad J. Improved pharmacokinetics and antihyperlipidemic efficacy of rosuvastatin-loaded nanostructured lipid carriers. J. Drug. Target. 2017;25(1):58–74.
30. Haripriyaa M, Suthindhiran K. Pharmacokinetics of nanoparticles: current knowledge, future directions and its implications in drug delivery. Futur. J. Pharm. Sci. 2023;9(113):1-26.
31. Jenning V, Thunemann AF, Gohla SH. Characterisation of a novel solid lipid nanoparticles carrier system based on binary mixtures of liquid and solid lipids. Int. J. Pharm. 2000;199:167-77.
32. Fuentes MG, Torres D, Alonso MJ. Design of lipid nanoparticles for the oral delivery of hydrophilic macromolecules. Colloids Surf. B Biointerfaces. 2003;27:159-68.
33. Nayak AP, Tiyaboonchai W, Patankar S, Madhusudhan B, Souto EB. Curcuminoids-loaded lipid nanoparticles: novel approach towards malaria treatment. Colloids Surf. B Biointerfaces. 2010;81:263–73.
34. Dolatabadi S, Karimi M, Nasirizadeh S, Hatamipour M, Golmohammadzadeh S, Jaafari MR. Preparation, characterization and *in vivo* pharmacokinetic evaluation of curcuminoids-loaded solid lipid nanoparticles (SLNs) and nanostructured lipid carriers (NLCs). J. Drug Deliv. Sci. Technol. 2021;62:1-10.

35. Das S, Ng WK, Kanaujia P, Kim S, Tan RBH. Formulation design, preparation and physicochemical characterizations of solid lipid nanoparticles containing a hydrophobic drug: Effects of process variables. Colloids Surf. B Biointerfaces. 2011; 88(1):483-9.
36. Mehnert W, Mäder K. Solid lipid nanoparticles: Production, characterization and applications. Adv. Drug. Deliv. Rev. 2001;47:165-96.
37. Dudhipala N, Janga KY, Gorre T. Comparative study of nisoldipine-loaded nanostructured lipid carriers and solid lipid nanoparticles for oral delivery: preparation, characterization, permeation and pharmacokinetic evaluation. Artif. Cells Nano-med. Biotechnol. 2018;46(S2):S616–S625.
38. Mathur P, Sharma S, Rawal S, Patel B, Patel MM. Fabrication, optimization, and *in vitro* evaluation of docetaxel-loaded nanostructured lipid carriers for improved anticancer activity. J. Liposome Res. 2020;30(2):182–96.
39. Souza LG, Silva EJ, Martins ALL, Mota MF, Braga RC, Lima EM, et al. Development of topotecan loaded lipid nanoparticles for chemical stabilization and prolonged release. Eur. J. Pharm. Biopharm. 2011;79(1):189–96.
40. Zhang C, Peng F, Liu W, Wan J, Wan C, Xu H, et al. Nanostructured lipid carriers as a novel oral delivery system for triptolide: induced changes in pharmacokinetics profile associated with reduced toxicity in male rats. Int. J. Nanomed. 2014;9:1049–63.